Broadband mid-IR frequency comb with CSP and AGS from a Er,Tm:Ho fiber laser

D. Sánchez[1,*], M. Hemmer[1], M. Baudisch[1], K. Zawilski[2], P. Schunemann[2], H. Hoogland[3,4], R. Holzwarth[3], and J. Biegert[1,5]

[1]*ICFO-Institut de Ciencies Fotoniques, Mediterranean Technology Park, 08860 Castelldefels (Barcelona), Spain*
[2]*BAE Systems, MER15-1813, P.O. Box 868, Nashua, New Hampshire 03061, USA*
[3]*Menlo Systems GmbH, Am Klopferspitz 19a, 82152 Martinsried, Germany*
[4]*Department of Physics, Friedrich-Alexander University Erlangen, 91058 Erlangen, Germany*
[5]*ICREA - Institució Catalana de Recerca i Estudis Avancats (ICREA), 08010 Barcelona, Spain*
**Corresponding author: daniel.sanchez@icfo.eu*

We report on the generation of a 2500 nm bandwidth frequency comb at 6.5 μm central wavelength from critically phase matched parametric downconversion in the nonlinear crystal $CdSiP_2$ (CSP) from a compact Er,Tm:Ho fiber laser. The generated ultra-broadband pulses show a transform-limited duration of 2.3 optical cycles and carry up to 85 pJ of energy at 100 MHz repetition rate. For comparison, the spectrum generated in AGS spans from 6.2 to 7.4 μm at FWHM with pulse energy of 3 pJ. A full 3D nonlinear wave propagation code is used for optimization of the noncollinear angle, propagation direction and crystal thickness.

For decades, the mid-IR spectral region ($3 < \lambda < 8$ μm) has been of interest owing to the numerous vibrational and rotational molecular resonances occurring in this spectral range [1,2]. The emergence of frequency comb technologies applied to this spectral range [3,4] has revealed the relevance of mid-IR ultra-broadband coherent sources as an enabling tool for high precision molecular spectroscopy [5,6]. mid-IR sources derived from difference frequency generation (DFG) from a common modelocked oscillator are of particular interest since such architecture directly provides a frequency stabilized comb [7,8]. In the temporal domain, these ultra-broadband stabilized mid-IR frequency combs translate into carrier-envelope phase (CEP) stable few-cycle pulses, which, upon energy scaling, are highly relevant for strong-field physics and attosecond spectroscopy.

Mid-IR ultra-broadband radiation is typically achieved via parametric downconversion of near-IR laser sources due to the lack of mature laser gain media with emission in the mid-IR. A number of mid-IR frequency comb sources have recently been reported featuring widely tunable outputs [9–11] in both the picosecond and femtosecond regime [12]. A challenge for direct frequency comb generation, especially from fiber laser sources, is however the low spectral brightness due to DFG in the nonlinear medium.

In this Letter, we demonstrate an ultra compact Er,Tm:Ho fiber laser frequency comb source based on $CdSiP_2$ (CSP) which achieves 85 pJ pulse energy in the spectral range from 5.5 to 8 μm. We compare the performance of CSP to the well-established $AgGaS_2$ (AGS) crystal and show that CSP achieves a near order of magnitude improvement over previous results.

The experimental setup consists of a fiber laser operating at 100 MHz and delivering phase-coherent femtosecond optical pulses at 1.55 μm and 2.03 μm wavelength (Menlo Systems GmbH [13]), a free-space Martinez-type assembly to temporally compress the 2 μm pulses [13] and a nonlinear crystal (Fig.1). The fiber laser outputs at 1.5 and 2 μm are used, respectively, as the pump and signal for the DFG. These outputs are spectrally and temporally characterized experimentally using second harmonic frequency-resolved optical gating. The measured and retrieved spectra, along with the corresponding retrieved temporal profiles are shown in Fig. 2. Both outputs originate from a single modelocked Er oscillator followed by amplification in Er and Tm:Ho based fiber amplifiers.

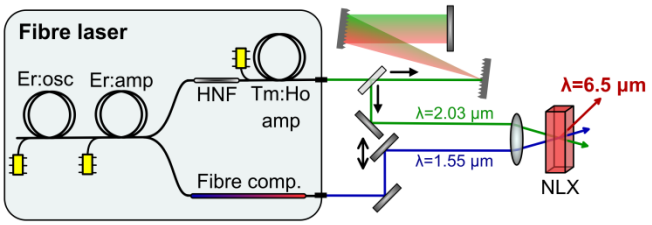

Fig. 1. Experimental setup showing the fiber laser system, the Martinez compressor and nonlinear crystal; HNF: highly nonlinear fiber, NLX: nonlinear crystal (CSP or AGS).

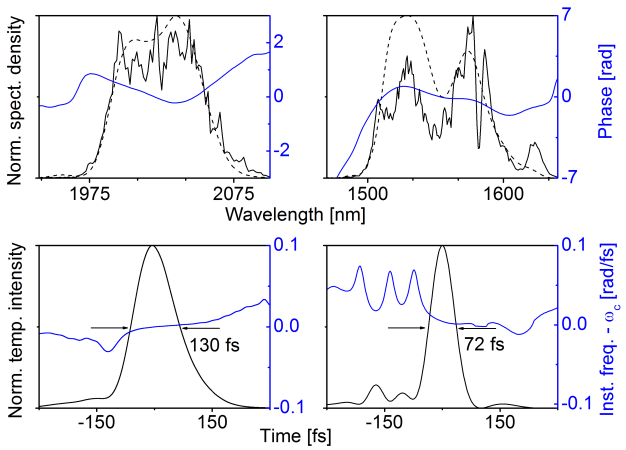

Fig. 2. Measured spectrum and reconstructed temporal profile from the FROG measurement of the signal (left column) and pump (right column). (Top) Retrieved phase (blue line), measured (black line) and retrieved (dashed black line) spectra. (Bottom) Retrieved temporal profile (black line) and instantaneous frequency (blue line).

The pump, centered at 1.55 µm wavelength, shows an average power of 350 mW. The pump pulses are compressed in the fiber system to 72 fs duration. The signal beam, centered at 2.03 µm wavelength exhibits an average power of 300 mW and uncompressed pulses with 25 ps duration. A free space Martinez-type folded compressor featuring a 360 l/mm grating and a 30 cm focal length Au-coated curved mirror with a throughput of 32% is used to compress the signal pulses down to 130 fs (95% of the transform limit). The pump and seed beams are focused using a single uncoated 40 mm focal length CaF_2 lens. Temporal overlap is ensured by inserting a delay line in the signal (2.03 µm) beam path. The generated mid-IR radiation is collimated using a 50 mm focal length CaF_2 lens and the optical power in the idler beam can be measured directly on a thermal sensor. The idler spectrum is measured with a Fourier transform IR (FTIR) spectrometer equipped with a liquid nitrogen cooled HgCdTe (MCT) detector.

The choice of nonlinear crystal is a critical aspect of this setup. Common oxide crystals are limited in transparency to around 4 µm, making it necessary to resort to non-oxyde nonlinear crystals. Ideally, the crystal needs to exhibit a transparency range accommodating the pump (1.55 µm), signal (2.03 µm) and idler (5-9 µm) waves and ideally also be transparent at the second harmonic of the pump wavelength (0.75 µm) to prevent two-photon absorption. Some of the more widely used mid-IR crystals such as $AgGaS_2$, $AgGaSe_2$ and GaSe as well as the newer lithium based crystals $LiGaS_2$, $LiGaSe_2$, $LiInS_2$ and $LiInSe_2$ satisfy this condition but exhibit either low nonlinearity ($LiGaS_2$, $LiGaSe_2$, $LiInS_2$, $LiInSe_2$) or unfavorable thermo-mechanical properties (GaSe, $AgGaS_2$ and $AgGaSe_2$). The newly developed negative uniaxial crystal CSP [14] is a promising alternative to these crystals due to its remarkably high effective nonlinear coefficient (as high as d_{eff}= 84.5 pm/V) as well as good thermal conductivity and phase matching abilities. In terms of d_{eff}, CSP outperforms all the crystals mentioned above and the transparency range that spans from 0.5 µm to 9 µm can comfortably accommodate our pump, signal and idler spectra for both linear and two-photon absorption. CSP has already shown great potential for downconversion to the mid-IR in non-critically phase matched schemes [15,16], yielding high efficiency in limited bandwidth (100-200 nm). However broader bandwidth could be achieved using a critically phase-matched configuration. Based on these considerations we chose CSP as a nonlinear crystal and performed in parallel a reference study in the same numerical and experimental conditions using AGS.

In order to investigate the potential of critical phase matching and to optimize the geometric configuration of the DFG and the thickness of the nonlinear crystals, a full 3D nonlinear wave propagation code [17] is used to simulate the down-conversion process in both CSP and AGS. This code accounts for all the relevant phenomena involved, such as temporal and spatial walk-off, noncollinear geometry, linear and two-photon absorption, etc, and has a proven ability for modeling complex laser systems [18]. The input pulses are modeled spectrally and temporally based on the experimental characterization reported in Fig. 2. The simulations suggest that in order to take full advantage of the bandwidth provided by the pump and seed pulses it is necessary to resort to noncollinear geometry in both crystals. According to our simulations, in the case of CSP the broadest phase matching is obtained for a propagation direction of the signal at $\theta = 66.5°$ with respect to the optical axis and an internal noncollinear angle between the signal and the pump of α = 1.85° for Type I (e-o=o) interaction. The optimum crystal thickness is determined by studying the evolution of the idler bandwidth and energy with propagation distance (Fig. 3).

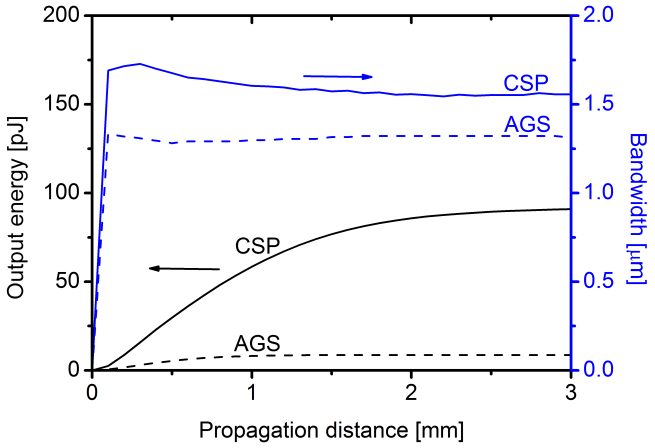

Fig. 3. Simulated evolution of the idler pulse energy (black line) and bandwidth at FWHM (blue line) as a function of propagation distance in the CSP (solid line) and AGS (dashed line) crystals.

The simulations show that the idler pulse energy increases linearly while the bandwidth slightly decreases over the first 2 mm of propagation, after which the combined effect of temporal and spatial walk-off as well as the noncollinear geometry cause both quantities to remain constant as the overlap of the pump and seed is reduced. In addition, the noncollinear geometry causes the idler beam profile to be increasingly oval with propagation distance. Taking these results into account, the crystal thickness is set to 1.5 mm as a tradeoff between optimum energy, bandwidth and beam profile. The simulations predict an idler pulse energy of approximately 75 pJ and over 1500 nm of bandwidth at FWHM. In the case of AGS, a larger noncollinear angle and group velocity mismatch cause the effective interaction length to be limited to around 1 mm. According to our simulations, the broadest phase matching configuration can be obtained for a cut angle of $\theta = 49.5°$ for Type II (e-o=e) interaction with an internal noncollinear angle of $\alpha = 2.1°$.

The CSP crystal is uncoated and cut at $\theta = 66.5°$ for Type I (e-o=o) interaction with an internal noncollinear angle of $\alpha = 1.85°$. The crystal is 1.5 mm in length with an aperture of 5 x 6 mm². The AGS crystal is AR coated for 1.5 µm, 1 mm thick and cut at $\theta = 49.5°$ for Type II (e-o=e) interaction with an internal noncollinear angle of $\alpha = 2.1°$. For both crystals, the pump and signal beams are focused to a measured FWHM diameter size of 44 µm. Tuning of the noncollinear angle is achieved by displacing the pump beam from the center of the focusing lens while keeping the input beams parallel to insure spatial overlap at the common focus.

We measured an average power of up to 8.5 mW (85 pJ) using CSP. The generated mid-IR radiation has central wavelength of 6.5 µm and exhibits a spectrum covering the spectral range from 5.5 to 8 µm supporting 50 fs transform-limited duration pulses, corresponding to 2.3 optical cycles (Fig. 4 - top). Some absorption in the collimating CaF_2 lens and optical components in the FTIR spectrometer is expected on the long wavelength side of the idler spectrum. The propagation distance of the idler pulse in CaF_2 is estimated to be 2 cm and the simulated spectrum corrected for absorption is shown in Fig. 4 (dashed blue line). Comparison of the measured and simulated spectra shows the excellent agreement between theory and experiment. Using AGS we measured an average power of only 300 µW (3 pJ). Even though we expected a lower output power from AGS due to its comparatively low nonlinearity, we believe that absorption of the mid-IR radiation in the AR coating is the main cause for the deviation from the predicted value. The idler spectrum in this case is shown in Fig. 4 and exhibits a 500 nm narrower extent compared to CSP.

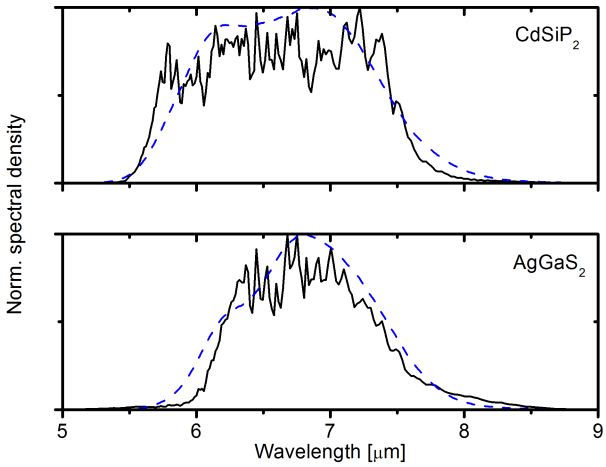

Fig 4. Measured idler spectrum (black, solid line) together with simulated spectrum (blue, dashed) based on numerical simulations of the DFG process including absorption in CaF_2. Top: CSP, Bottom: AGS.

In summary, we generated for the first time an ultra-broadband mid-IR frequency comb via noncollinear, non-critically phase-matched DFG in CSP. Comparison of the performance of the new CSP crystal compared to the well-established AGS crystal highlighted the superiority of CSP and resulted in a frequency comb covering the spectral range from 5.5 to 8 µm with 85 pJ energy content at a 100 MHz repetition rate and supporting a 2.3 optical cycles transform limit. The uniform flat-top like spectral intensity profile generated in CSP is particularly beneficial for applications in which a uniform spectral energy density is desirable, such as broadband spectroscopy. In addition, the high energy obtained from CSP make this all fiber Er,Tm:Ho source suitable for seeding a mid-IR optical parametric chirped pulse amplifier (OPCPA), where a higher seed energy leads to increased stability as well as relaxing the gain requirements on the optical parametric amplification stages. Future work may include increasing DFG seed energies for direct measurement of the CEP and pulse duration in the mid-IR.

We acknowledge support from MINISTERIO DE ECONOMÍA Y COMPETITIVIDAD through Plan Nacional (FIS2011-30465-C02-01), the Catalan Agencia de Gestio d'ajuts Universitaris i de Recerca (AGAUR) with SGR 2014-2016, Fundacio Cellex Barcelona, funding from LASERLAB-EUROPE, grant 228334, the German BMBF for funding under the Eurostars project MIRANDUS and the European Union through FP7 Marie Curie actions project CCQED.

References

1. F. K. Tittel, D. Richter, and A. Fried, Top. Appl. Phys. **89**, 458–529 (2003).
2. W. Petrich, Appl. Spectrosc. Rev. **36**, 181–237 (2001).

3. J. Reichert, R. Holzwarth, T. Udem, and T. W. Hänsch, Opt. Commun. 59–68 (1999).
4. S. A. Diddams, J. Opt. Soc. Am. B **27**, 51–63 (2010).
5. A. Schliesser, N. Picqué, and T. W. Hänsch, Nat. Photonics **6**, 440–449 (2012).
6. A. Hugi, G. Villares, S. Blaser, H. C. Liu, and J. Faist, Nature **492**, 229–233 (2012).
7. A. Baltuska, T. Fuji, and T. Kobayashi, Phys. Rev. Lett. **88**, 133901 (2002).
8. T. Fuji, A. Apolonski, and F. Krausz, Opt. Lett. **29**, 632–635 (2004).
9. C. Erny, K. Moutzouris, J. Biegert, D. Kühlke, F. Adler, A. Leitenstorfer, and U. Keller, Opt. Lett. **32**, 1138–1140 (2007).
10. A. Ruehl, A. Gambetta, I. Hartl, M. E. Fermann, K. S. E. Eikema, and M. Marangoni, Opt. Lett. **37**, 2232–2235 (2012).
11. A. Gambetta, N. Coluccelli, M. Cassinerio, D. Gatti, P. Laporta, G. Galzerano, and M. Marangoni, Opt. Lett. **38**, 1155–1157 (2013).
12. M. Beutler, I. Rimke, E. Büttner, V. Petrov, and L. Isaenko, Opt. Lett. **39**, 4353–4355 (2014).
13. H. Hoogland, A. Thai, D. Sanchez, S. L. Cousin, M. Hemmer, M. Engelbrecht, J. Biegert, and R. Holzwarth, Opt. Express **21**, 31390–31394 (2013).
14. K. T. Zawilski, P. G. Schunemann, T. C. Pollak, D. E. Zelmon, N. C. Fernelius, and F. K. Hopkins, J. Cryst. Growth **312**, 1127–1132 (2010).
15. O. Chalus, P. G. Schunemann, K. T. Zawilski, J. Biegert, and M. Ebrahim-Zadeh, Opt. Lett. **35**, 4142–4144 (2010).
16. Z. Zhang, D. T. Reid, C. K. Suddapalli, P. G. Schunemann, K. T. Zawilski, and C. R. Howle, Opt. Lett. **38**, 5110–5113 (2013).
17. G. Arisholm, J. Opt. Soc. Am. B **14**, 2543–2549 (1997).
18. A. Thai, C. Skrobol, P. K. Bates, G. Arisholm, Z. Major, F. Krausz, S. Karsch, and J. Biegert, Opt. Lett. **35**, 3471 (2010).

1. F. K. Tittel, D. Richter, and A. Fried, "Mid-Infrared laser applications in spectroscopy," Top. Appl. Phys. **89**, 458–529 (2003).
2. W. Petrich, "Mid-Infrared and Raman spectroscopy for medical diagnostics," Appl. Spectrosc. Rev. **36**, 181–237 (2001).
3. J. Reichert, R. Holzwarth, T. Udem, and T. W. Hänsch, "Measuring the frequency of light with mode-locked lasers," Opt. Commun. 59–68 (1999).
4. S. A. Diddams, "The evolving frequency comb," J. Opt. Soc. Am. B **27**, 51–63 (2010).
5. A. Schliesser, N. Picqué, and T. W. Hänsch, "Mid-infrared frequency combs," Nat. Photonics **6**, 440–449 (2012).
6. A. Hugi, G. Villares, S. Blaser, H. C. Liu, and J. Faist, "Mid-infrared frequency comb based on a quantum cascade laser," Nature **492**, 229–233 (2012).
7. A. Baltuska, T. Fuji, and T. Kobayashi, "Controlling the carrier-envelope phase of ultrashort light pulses with optical parametric amplifiers," Phys. Rev. Lett. **88**, 133901 (2002).
8. T. Fuji, A. Apolonski, and F. Krausz, "Self-stabilization of carrier-envelope offset phase by use of difference-frequency generation," Opt. Lett. **29**, 632–635 (2004).
9. C. Erny, K. Moutzouris, J. Biegert, D. Kühlke, F. Adler, A. Leitenstorfer, and U. Keller, "Mid-infrared difference-frequency generation of ultrashort pulses tunable between 3.2 and 4.8 mm from a compact fiber source," Opt. Lett. **32**, 1138–1140 (2007).
10. A. Ruehl, A. Gambetta, I. Hartl, M. E. Fermann, K. S. E. Eikema, and M. Marangoni, "Widely-tunable mid-infrared frequency comb source based on difference frequency generation," Opt. Lett. **37**, 2232–2235 (2012).
11. A. Gambetta, N. Coluccelli, M. Cassinerio, D. Gatti, P. Laporta, G. Galzerano, and M. Marangoni, "Milliwatt-level frequency combs in the 8-14 um range via difference frequency generation from an Er:fiber oscillator," Opt. Lett. **38**, 1155–1157 (2013).
12. M. Beutler, I. Rimke, E. Büttner, V. Petrov, and L. Isaenko, "Difference-frequency generation of fs and ps mid-IR pulses in LiInSe2 based on Yb-fiber laser pump sources," Opt. Lett. **39**, 4353–4355 (2014).
13. H. Hoogland, A. Thai, D. Sanchez, S. L. Cousin, M. Hemmer, M. Engelbrecht, J. Biegert, and R. Holzwarth, "All-PM coherent 2.05 μm Thulium/Holmium fiber frequency comb source at 100 MHz with up to 0.5 W average power and pulse duration down to 135 fs," Opt. Express **21**, 31390–31394 (2013).
14. K. T. Zawilski, P. G. Schunemann, T. C. Pollak, D. E. Zelmon, N. C. Fernelius, and F. K. Hopkins, "Growth and characterization of large CdSiP2 single crystals," J. Cryst. Growth **312**, 1127–1132 (2010).
15. O. Chalus, P. G. Schunemann, K. T. Zawilski, J. Biegert, and M. Ebrahim-Zadeh, "Optical parametric generation in CdSiP2," Opt. Lett. **35**, 4142–4144 (2010).
16. Z. Zhang, D. T. Reid, C. K. Suddapalli, P. G. Schunemann, K. T. Zawilski, and C. R. Howle, "Femtosecond-laser pumped CdSiP2 optical parametric oscillator producing 100 MHz pulses centered at 6.2 μm," Opt. Lett. **38**, 5110–5113 (2013).
17. G. Arisholm, "General numerical methods for simulating second-order nonlinear interactions in birefringent media," J. Opt. Soc. Am. B **14**, 2543–2549 (1997).
18. A. Thai, C. Skrobol, P. K. Bates, G. Arisholm, Z. Major, F. Krausz, S. Karsch, and J. Biegert, "Simulations of petawatt-class few-cycle optical-parametric chirped-pulse amplification, including nonlinear refractive index effects," Opt. Lett. **35**, 3471 (2010).